**Supplemental Figures**

# Linking epigenetic dysregulation, mitochondrial impairment, and metabolic dysfunction in SBMA motor neurons

Naemeh Pourshafie, Ester Masati, Eric Bunker, Alec R. Nickolls, Parisorn Thepmankorn, Kory Johnson, Xia Feng, Tyler Ekins, Christopher Grunseich, and Kenneth H. Fischbeck

Supplementary Figure 1

A

| iPSC lines | (CAG)n | hNIL insertion tool |
|---|---|---|
| SB1 | 51 | TALEN |
| SB3 | 51 | TALEN |
| SB15 | 54 | TALEN |
| SB17 | 53 | CRISPR |
| WTC11 | Wildtype | TALEN |
| HT179 | Wildtype | CRISPR |
| HT180 | Wildtype | TALEN |
| HT180ARKO | AR knock out | TALEN |
| SB18ARKO | AR knock out | TALEN |

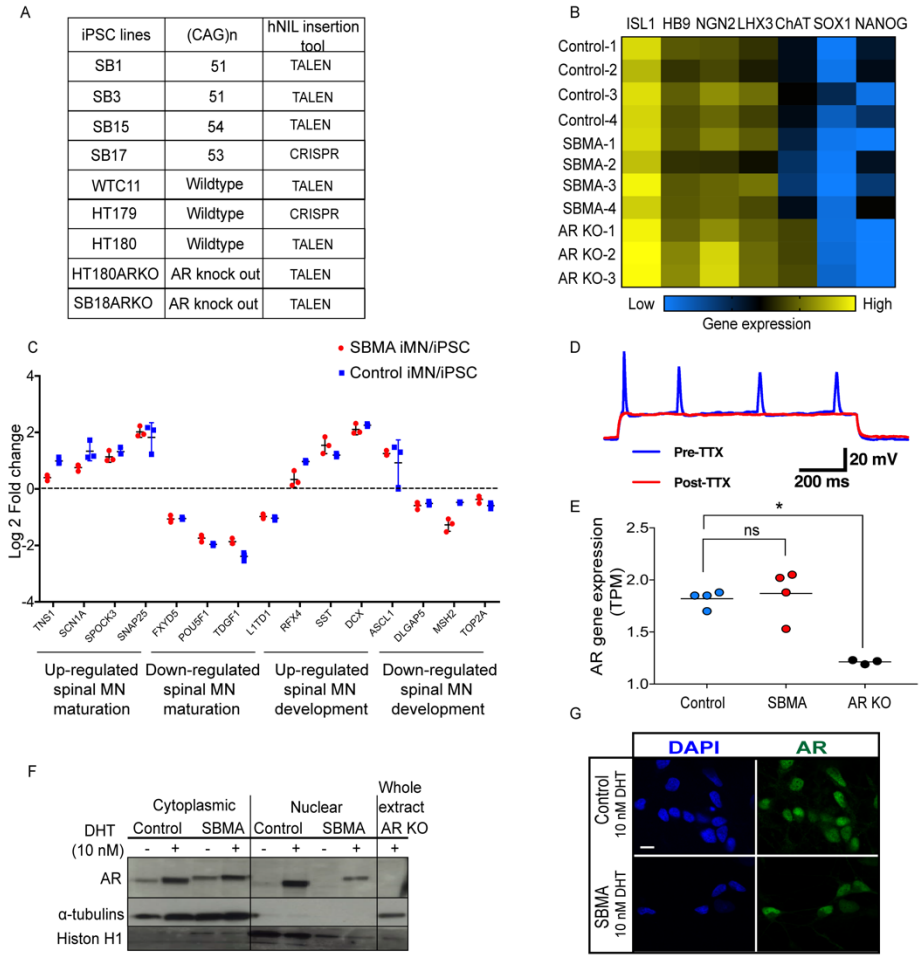

**Supplemental Figure 1. Characterization of iMNs differentiated from SBMA iPSCs**

(A) List of iPSCs transfected with the hNIL cassette by TALEN or CRISPR/Cas9-mediated integration. Cell lines used for RNA-sequencing are highlighted in red. Asterisk represents cell lines that were used as replicate samples for RNA-sequencing. (B) Heatmap summary of RNA-seq analysis of iMNs showing expression of motor neuron genes and repression of SOX2 and Nanog, across biological replicates (N=3, n=1 SBMA, N=2, n=2 controls; N=3 AR KO iMNs). (C) qRT-PCR analysis of 15 genes previously selected to represent spinal motor neuron maturation and development. Data normalized to GAPDH expression. (D) Whole-cell patch clamp recording of control iMNs (28 dpi). (E) Transcript per million (TPM) values of AR gene from RNA-seq analysis. RNA-seq was performed on biological replicates (N=3, n=1 SBMA, N=2, n=2 controls; n=3 AR KO iMNs). *$p < 0.05$, one-way ANOVA followed by Bonferroni's multiple comparisons test. (F) Representative western blot showing expression and nuclear localization of AR with 10 nM DHT treatment. (G) Representative images of AR localization in the nucleus in iMNs treated with 10 nM DHT. DAPI (blue) and AR (green). Scale bar, 10 μm. The iMNs were treated with 10 nM DHT. Related to Figure 1.

Supplementary Figure 2

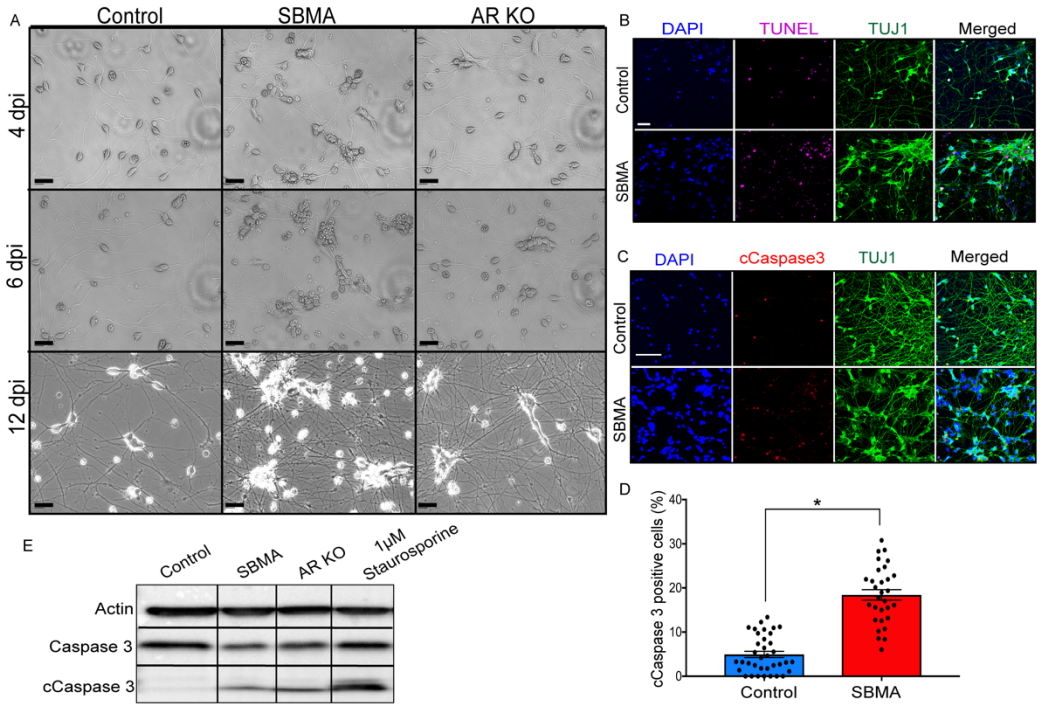


**Supplemental Figure 2. SBMA iMNs degenerate over time**

(A) Representative brightfield images of iMNs at different time points showing increased clumping and cell death. Scale bar, 40 μm. (B) Representative images of apoptotic iMNs (6dpi) by TUNEL assay. Apoptotic cells (purple) and Hoechest (blue). Scale bar, 100 μm. (C) Immunostaining of DAPI (blue), cCaspase3 (red), and TUJ1 (green) of iMNs (6dpi). Scale bar, 100 μm. (D) Percentage of cCaspase 3 positive cells in whole cultures, assessed by immunostaining (N=3 SBMA and N=3 control); error bars show mean ± SE, *$p < 0.05$, two-tailed Student's *t*-test. (E) Western blot analysis of cCaspase3 and caspase 3 in iMNs (6dpi). Control iMNs treated with 1 μM treated staurosporine were used as a positive control. Actin was used as a loading control. The iMNs were treated with 10 nM DHT. Related to Figure 1.

Supplemental Figure 3

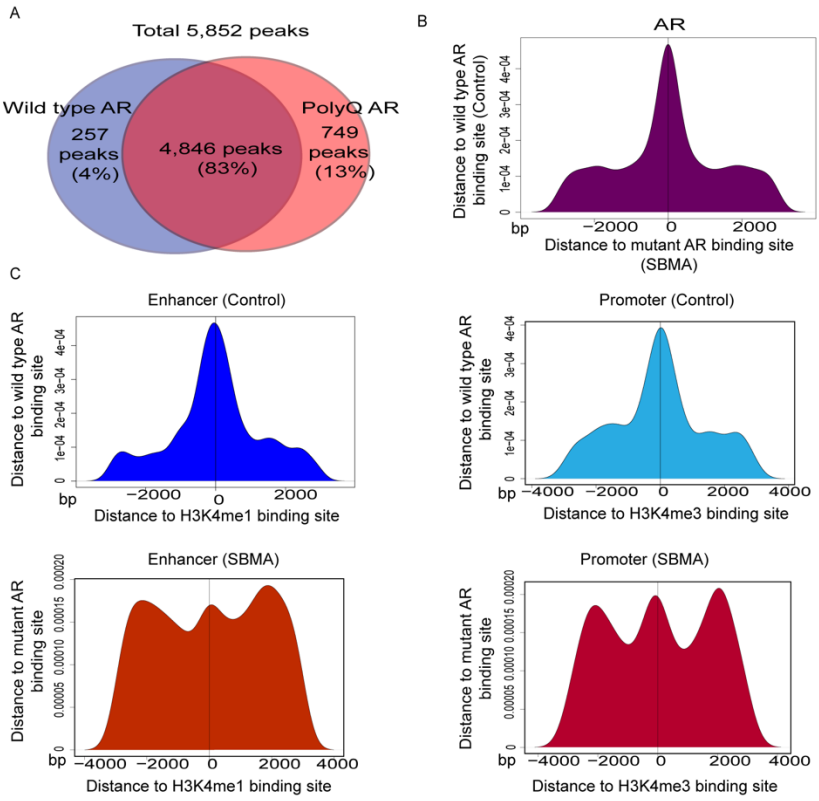


**Supplemental Figure 3. PolyQ and wild type AR co-occurrence with promoter and enhancer regions differs in control and SBMA iMNs**

**(A)** AR ChIP-sequencing resulted in 5,852 peaks in both coding and non-coding regions across 3 SBMA and 3 control iMNs. All peaks normalized to negative control (AR KO). **(B)** Co-occupancy of wild type AR signals over a scaled window of ±3 kb of the polyQ AR peak. **(C)** Co-occupancy of wildtype AR (top) and polyQ AR (bottom) around H3K4me1- and H3K4me3-occupied regions (measured by ChIP-seq). The iMNs were treated with 10 nM DHT. Related to Figure 2.

Supplemental Figure 4

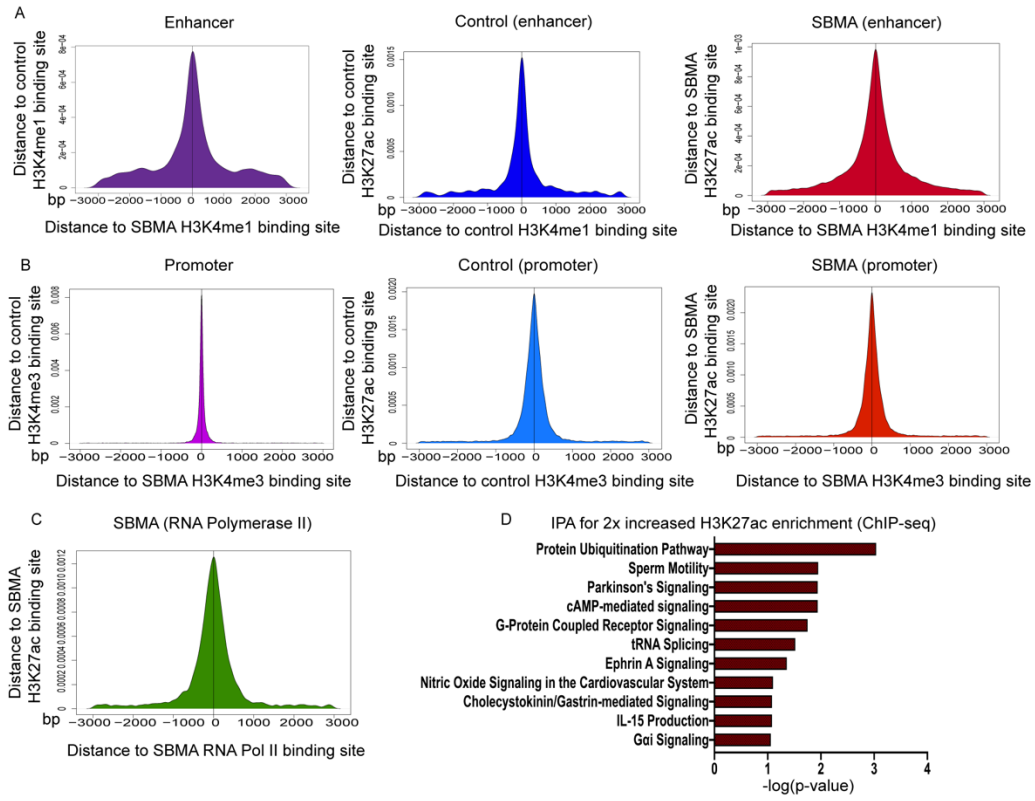


**Supplemental Figure 4. H3K27ac co-occurrence with promoter and enhancer regions**

(A-B) H3K27ac peaks co-occurred around H3K4me1- and H3K4me3-occupied regions, in both SBMA and control iMNs (measured by ChIP-seq). The H3K27ac signal is shown over a scaled window of ±3 kb of the AR peak. (C) H3K27ac peak distribution near RNA Pol II peaks in SBMA iMNs (measured by ChIP-seq). The H3K27ac signal is shown over a scaled window of ±3 kb from the AR peak. (D) Ingenuity pathway analysis of genes with greater than 2-fold H3K27ac binding. The iMNs were treated with 10 nM DHT. Related to Figure 2 and 3.

Supplemental Figure 5

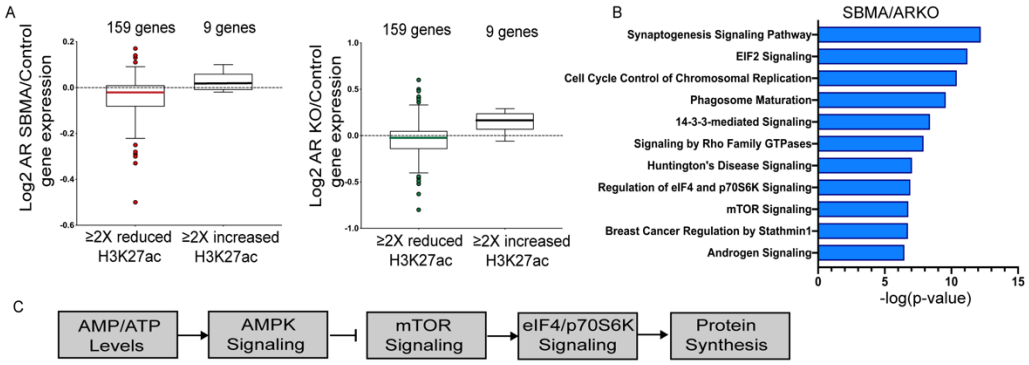


**Supplemental Figure 5. Dysregulation of mTOR signaling pathway indicates perturbed energy homeostasis**

(A) Expression changes of noise-filtered genes from RNA-seq data with greater than 2-fold reduced H3K27ac (159 genes) or greater than 2-fold increased H3K27ac (9 genes). (B) IPA of genes identified as having significant expression differences in SBMA over AR KO iMNs (RNA-seq). (N=3, n=1 SBMA, N=2, n=2 controls; N=3 AR KO iMNs). Fold change >1.5 and corrected p-value <0.05. (C) A simplified schematic of the AMPK/mTOR pathway. In response to low ATP levels, activated AMPK inhibits mTOR signaling. Elevated ATP inactivates AMPK and promotes mTOR signaling. The iMNs were treated with 10 nM DHT.

Supplementary Figure 6

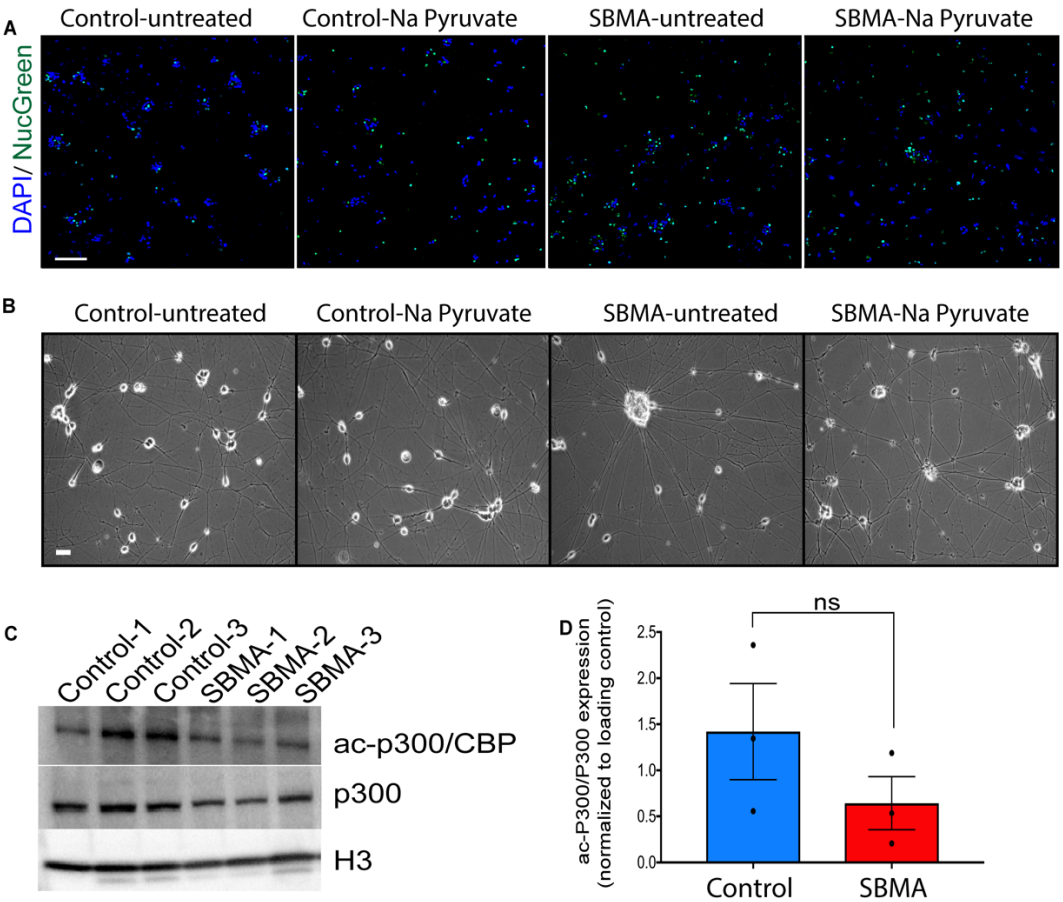


**Supplemental Figure 6. Sodium pyruvate increases SBMA iMN viability**

(A) Representative images of dying cells that lost plasma membrane integrity were detected with a florescent stain in real time (6dpi). NucGreen dead 488 (Green) and DAPI (blue). Scale bar, 50 μm. (B) Representative brightfield images of iMNs treated with 20 mM sodium pyruvate at 6dpi. SBMA iMNs show less cell clumping with treatment. Scale bar, 40 μm. (C) Acetylated P300/CBP (ac-P300/CBP) immunoblot analysis of protein lysates from iMNs. H3 was used as a loading control. (D) Western blot quantification showing ac-p300/P300 ratio, normalized to H3 loading control. All experiments were performed on N=3 SBMA and N=3 control. Error bars show mean ± SE, two-tailed Student's *t*-tests. The iMNs were treated with 10 nM DHT. Related to Figure 5.

Supplemental Figure 7

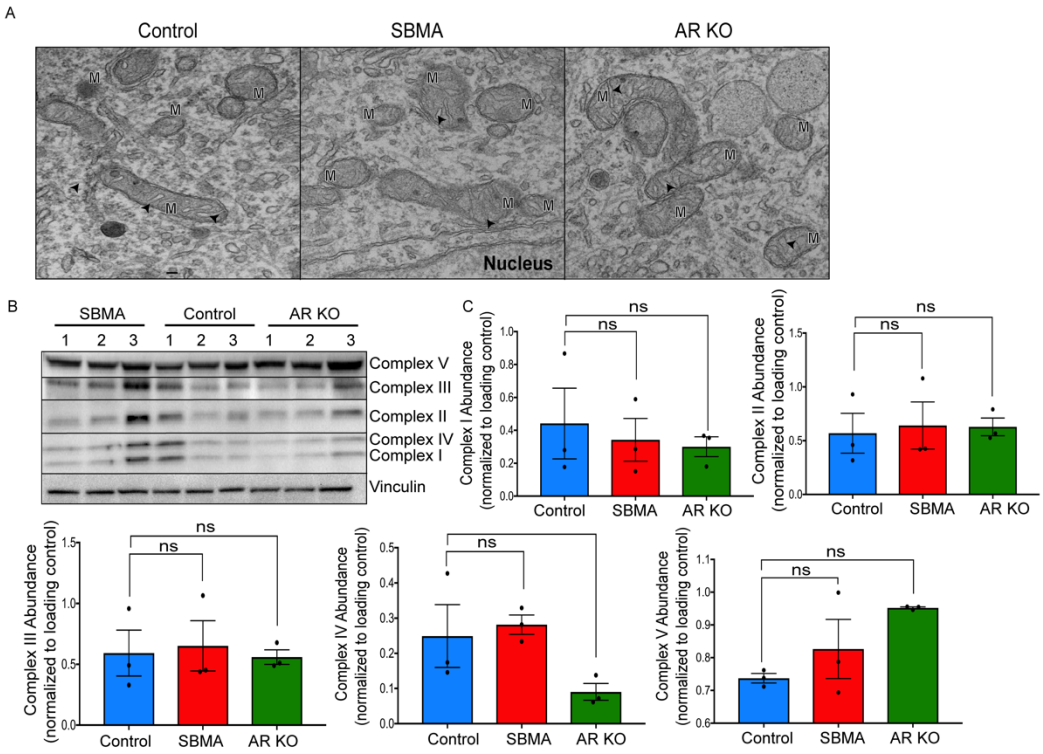


**Supplemental Figure 7. Preserved mitochondrial morphology and ETC integrity in SBMA iMN**

(A) Electron microcopy (EM) characterization of mitochondrial morphology, matrix density and cristae shape (arrowheads). Scale bar, 100 μm. (B) ETC immunoblot analysis of protein lysates from iMNs. Vinculin was used as a loading control. All experiments were performed on N=3 SBMA, N=3 control, and N=3 AR KO. (C) Quantification of western blot analysis of ETC complex showing no significant change in the expression of the 5 ETC protein complexes (NDUFB8, SDHD, UQCRC2, MT-COI and ATP5A) in SBMA, control and AR KO iMNs. Vinculin was used as a loading control. Error bars show mean ± SE. One-way ANOVA followed by Bonferroni's multiple comparisons test. The iMNs were treated with 10 nM DHT. Related to Figure 5.